

Rollover Prevention Based on the Relation between Motion and Position of the Center of Gravity

Kailun Yu and Yutaka Watanabe

Department of Logistics and Information Engineering, Tokyo University of Marine Science and Technology, Tokyo 1358533, Japan

Abstract: Rollover is a serious kind of road accident. Such accidents frequently happen on sections of curved roads because of the external lateral force: centrifugal force. High COG (center-of-gravity) objects such as trucks and SUVs (sport utility vehicles) are more prone to rollover. This research specifically examines the relation between motions and the COG position. The height and the maximum height of COG are calculated using natural motion frequencies of a moving object, based on the method using D3DCG (detection of the three-dimensional center of gravity). Furthermore, the maximum lateral force the vehicle can withstand without rolling over can be calculated. It is the rollover criterion. Because of the different structures of vehicles, the rollover criterion is considered from two perspectives: natural vibration and geometric structure. Rollover prevention is achieved by comparing the real-time lateral force acting on a vehicle with the rollover criterion. A system to ascertain the autonomous cornering at the fastest speed that does not result in a rollover is created. The accuracy of this system is proved by experimentation with a remote-controlled car. Furthermore, the experiment demonstrates the possibility of applying this technology to autonomous driving.

Key words: Center of gravity, rollover prevention, trucks and SUVs, road accidents, traffic safety.

1. Introduction

The probability of a rollover accident is 5%, but the number of deaths caused by rollovers is as high as 30% of the total road traffic accident mortality rate [1]. After a rollover accident, only 2% of vehicles can leave the accident scene under their own power [2]. Tall and narrow vehicles such as SUVs (sport utility vehicles) are prone to rollover because of their instability, which is attributable to their high COG (center-of-gravity). Since 2000, SUV rollover accidents have accounted for 41.9% of all rollover accidents. In fact, rollover accidents often take place on sections of winding roads [3]: when a vehicle is rounding a corner, the external lateral force (centrifugal force) affects its COG [4, 5]. Rollover will happen if this force is very strong. Therefore, the position of the COG is an important factor affecting rollover [6].

To prevent rollover, many researchers have proposed various methods. Several common strategies are used to

prevent rollover accidents: TTR (Time-To-Rollover) [7], LTR (Load Transfer Ratio) [8], and the implementation of ARBs (Anti-Roll Bars) [9]. Zhu et al. [10] introduced an innovative integrated chassis control system aimed at mitigating vehicle rollover risks, particularly adopting neural network-based TTR warning indicators for enhanced prediction. The approach takes advantage of a back-propagation neural network tailored specifically for rollover anticipation. Furthermore, the study rigorously assessed the efficacy of algorithms designed to control the active yaw moment and active front steering in diverse, representative driving scenarios. Li et al. [11] described an IPLTR (improved predictive lateral load transfer ratio) as the rollover metric and achieved real-time calculation using an 8-DOF (degree-of-freedom) nonlinear vehicle model. Yim et al. [12] newly developed a rollover prevention controller that takes advantage of the ESP (electronic stability program) for proactive braking, aiming to mitigate vehicle speed and

Corresponding author: Yutaka Watanabe, Doctor of engineering, professor, research fields: transportation safety and the center of gravity detection.

lateral acceleration, while incorporating an AARB (active anti-roll bar) to bolster rollover prevention capabilities. Nevertheless, recent studies have overlooked the influence of the COG height on rollover phenomena [13]. Many researchers either assume a fixed value for the COG height [14], or employ methodologies to forecast unknown variables, inclusive of the COG height [15]. In doing so, procedures applied for computing rollover prevention can become complicated, leading to large errors.

2. Relation between Motion and the COG Position

The conventional method to detect a vehicle COG height uses a truck scale [16]. However, this method lacks flexibility and costs both time and money. Watanabe proposed the D3DCG (detection of the three-dimensional center of gravity) theory, which is an application of ship buoyancy principles: ships with different COG heights have different oscillation frequencies [17, 18]. Therefore, their heaving and rolling frequencies are useful to detect the COG height. When a vehicle is in motion, it encounters various road surface irregularities that induce vehicle's oscillations. The frequency of these oscillations is contingent upon the vehicle's COG location. Consequently, by analyzing the natural frequencies of the oscillations, the COG height can be detected.

Fig. 1 shows an oscillation sketch of a moving vehicle. The relation between motion and position of the COG can be expressed as

$$L^2 + \frac{g}{4\pi^2\nu^2}L - \frac{b^2\nu'^2}{4\nu^2} = 0 \quad (1)$$

where L represents the vertical separation from the oscillation center to the height of the COG, ν represents the horizontal shaking (rolling) frequency, ν' stands for the frequency of vertical simple harmonic oscillation (heaving), π is the circular constant, g stands for the acceleration of gravity, and b denotes the width of the total weight-bearing section.

Based on the equation above, the COG height can be

detected even with no knowledge of the total mass or spring constant. For each object, the COG height has a limitation. The object will roll over if its COG exceeds this limitation.

During vehicle oscillation, a restoring force (f) returns the vehicle body to its original position. The existence of the restoring force results from competition of the elastic moment and gravity moment. The expression for the rotational moment balance is

$$f = -\frac{m}{L} \left(\frac{kb^2}{2m} - gL \right) \sin \theta \quad (2)$$

where f stands for the restoring force perpendicular to the connecting line between the COG and oscillation center, k represents the elastic coefficient of spring, θ denotes the rolling angle, and m signifies the total mass.

To ensure that the vehicle will not roll over, the value of f must be no more than 0. Therefore, a formula exists as

$$\frac{kb^2}{2m} - gL \geq 0 \quad (3)$$

In the static condition, when f is 0, L reaches the maximum height of COG, denoted as L_{max} . According to Kawashima and Watanabe [19], the unknown variables m and k have the relation with heaving frequency of $k/m = 2\pi^2\nu'^2$. Consequently, the expression of L_{max} is

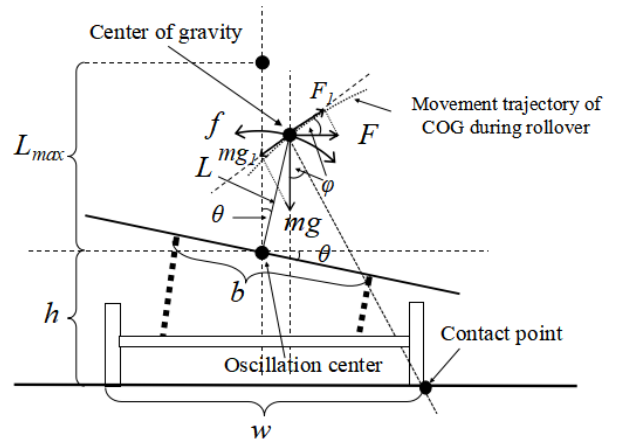


Fig. 1 Diagram of the rollover critical state between motion and position of COG.

$$L_{\max} = \frac{\pi^2 v'^2 b^2}{g} \quad (4)$$

3. Rollover Criterion

Merely being aware of COG height and its maximum threshold is insufficient to prevent rollover. Consequently, this study, grounded in the theories described above, meticulously examines the lateral force, presented as F , which affects the COG as a vehicle moves along a curving road. A particular challenge lies in the fact that various vehicle types possess distinct structural configurations. To address this challenge, two methodologies are introduced to approach the calculation of the critical rollover lateral force from two distinct perspectives: one incorporating natural vibration characteristics, and the other, geometric structural aspects. The result with the smaller value is subsequently selected as the rollover criterion.

3.1 Natural Vibration

For a vehicle to operate stably, the value of L must remain below that of L_{\max} . The gravitational potential energy of raising L to L_{\max} is converted into the kinetic energy of the oscillating vehicle and the elastic potential energy of springs. However, there exists a deflecting angle θ_{\max} , over which springs cannot restore the oblique vehicle body, even if all the gravitational potential energy is transformed into the springs' elastic potential energy.

In Fig. 1, based on the law of conservation of energy, the rollover critical state is

$$mg(L_{\max} - L) = \frac{1}{2}kb^2 \sin^2 \theta_{\max} \quad (5)$$

where θ_{\max} denotes the maximum deflecting angle without rollover.

Considering (4), θ_{\max} becomes

$$\theta_{\max} = \sin^{-1} \sqrt{\frac{L_{\max} - L}{L_{\max}}} \quad (6)$$

When a vehicle traverses a curve, the external lateral

force exerted upon it is presumed to be related to gravity as

$$F = qmg \quad (7)$$

where q stands for a multiple of lateral force in relation to gravity.

If a rollover is imminent, then the restoring force must equate to the lateral force component perpendicular to the line connecting the COG and the vibration center. This equivalence can be expressed mathematically as

$$f = qmg \cos \theta \quad (8)$$

As the vehicle body inclines to one side, springs of that side are compressed, whereas the springs on the opposite side experience extension. Consequently, the elastic moment's direction counteracts the direction of the deflection. Nevertheless, because of inertia, the gravity moment aligns with the direction of deflection.

By combining Equations (2) and (8) and by eliminating m and k by L_{\max} , q is expressed as

$$q = \left(-\frac{L_{\max}}{L} + 1 \right) \tan \theta \quad (9)$$

Here, because we consider q in terms of natural vibration, it is expressed as q_v . If θ attains its maximum value θ_{\max} , then q_v will reach its maximum multiple of lateral force $q_{v\max}$, which signifies the critical state of rollover from a natural vibration perspective. According to Equation (6), $q_{v\max}$ is

$$q_{v\max} = \left(-\frac{L_{\max}}{L} + 1 \right) \tan \left(\sin^{-1} \sqrt{\frac{L_{\max} - L}{L_{\max}}} \right) \quad (10)$$

3.2 Geometric Structure

Based on Equation (9), the real-time deflecting angle θ can be formulated in terms of the real-time variable q as

$$\theta = \tan^{-1} \left(\frac{Lq}{L - L_{\max}} \right) \quad (11)$$

Vehicles frequently exhibit varied structures. Occasionally, even when the deflecting angle fails to attain its maximum value θ_{\max} as specified in Equation (6), rollover can still occur because of the inherent geometric configuration of the vehicle. Under such circumstances, the rollover center corresponds to the contact point between the outer wheel and the surface of the road, as depicted in Fig. 1.

To prevent rollover, it is imperative that the lateral force component identified as F_1 in Fig. 1 and aligned with the tangent of the COG's movement trajectory, not surpass the gravitational force component expressed as mg_1 on the same axis. Thereby, we have

$$mg \sin \varphi \geq q_s mg \cos \varphi \quad (12)$$

where φ represents the angle formed by the vertical axis and the line linking the COG with the rollover center. Here, the lateral force is analyzed with respect to the vehicle's geometric structure. Consequently, q is denoted as q_s .

In light of the relation presented in Equation (12), upon reaching the critical state of rollover, the vehicle's q_s attains its peak value. This peak value situation can be mathematically represented as

$$q_{s\max} = \tan \varphi_{\min} \quad (13)$$

where $q_{s\max}$ stands for the maximum multiple of gravity that is sustainable without rollover from a geometric structure perspective. Also, $\tan \varphi_{\min}$ represents the minimum tangent value of angle φ .

According to the geometric structure of the vehicle presented in Fig. 1, $\tan \varphi$ can be expressed by rolling angle θ as

$$\tan \varphi = \frac{\frac{w}{2} - L \sin \theta}{L \cos \theta + h} \quad (14)$$

where w denotes the distance separating the outer edges of the wheels on both sides, and where h signifies the vertical distance between the ground and

the oscillation center.

In Equation (14), $\tan \varphi$ decreases as θ increases. In Equation (11), θ increases with the increase in q_s . Consequently, when q_s reaches the maximum value, $\tan \varphi$ achieves its minimum value. As a result, Equation (13) shows that the maximum multiple of the lateral force is represented as

$$q_{s\max} = \frac{\frac{w}{2} - L \sin \left[\tan^{-1} \left(\frac{L q_{\max}}{L - L_{\max}} \right) \right]}{L \cos \left[\tan^{-1} \left(\frac{L q_{\max}}{L - L_{\max}} \right) \right] + h} \quad (15)$$

The natural vibrations and geometric structures of different vehicles can be expected to differ. Therefore, this study applies a smaller value between $q_{v\max}$ and $q_{s\max}$ as the rollover criterion, denoted as q_{\max} . When the real-time multiple of lateral force q attains q_{\max} , the vehicle velocity corresponds to the highest cornering speed which can be achieved without inducing a rollover.

4. Introduction of the Experimental Scale Model and Control System

To verify the rollover criterion, experiments are conducted with a remote-controlled car as depicted in Fig. 2. A microcomputer and a motion sensor (200 Hz sampling rate) are installed on the car to calculate q_{\max} and to measure q in real time.

Because rollover occurs when $q \geq q_{\max}$, the criterion for evaluating the risk of the rollover is adopted as

$$\frac{q}{q_{\max}} \times 100(\%) \quad (16)$$

The microcomputer also works to control the accelerating DC motor and the steering servo motor of the car. The three-color LED (light-emitting diode) roughly displays the risk of the rollover according to the value of q/q_{\max} . After the acceleration and the steering angle of the car are sent to the microcomputer

by a PC (personal computer), q/q_{max} is sent back to the PC by the microcomputer through Wi-Fi communication. Consequently, the car can be controlled remotely by a control panel of the PC. Furthermore, the specific rollover risk is shown on the panel.

The control panel has two modes: one is to drive the car manually; the other is to drive the car autonomously. In manual control mode, the acceleration and direction of the car can be adjusted manually on the control panel. When in autonomous cornering mode, the car is assigned a random turning angle to execute. Then the speed increases gradually until it reaches the rollover criterion. Subsequently, it begins to decrease. When it

drops below the rollover criterion, it accelerates again. This process is repeated continuously, but rollover will not occur.

Feedback control of the autonomous cornering depicted in Fig. 2 is done according to a simple process explained roughly using the pseudo-code presented below.

1. Set the full angle of the steering.
2. Accelerate slightly, watching q/q_{max} .
3. If $q/q_{max} < 1$, then go to 2.
4. If $q/q_{max} \geq 1$, then decelerate slightly and incrementally until $q/q_{max} < 1$; go back to 2.

Consequently, the fastest autonomous cornering without rollover is achieved.

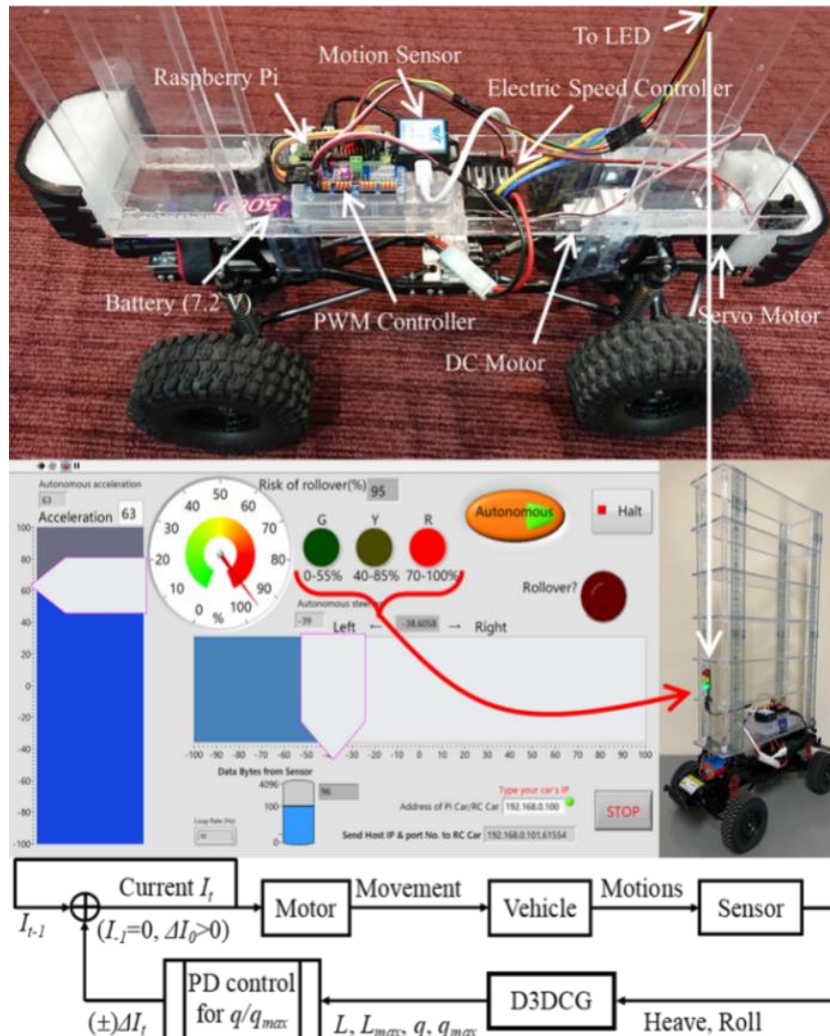


Fig. 2 Specifications of the experimental scale model, control panel on a PC, and a feedback control system for preventing rollover.

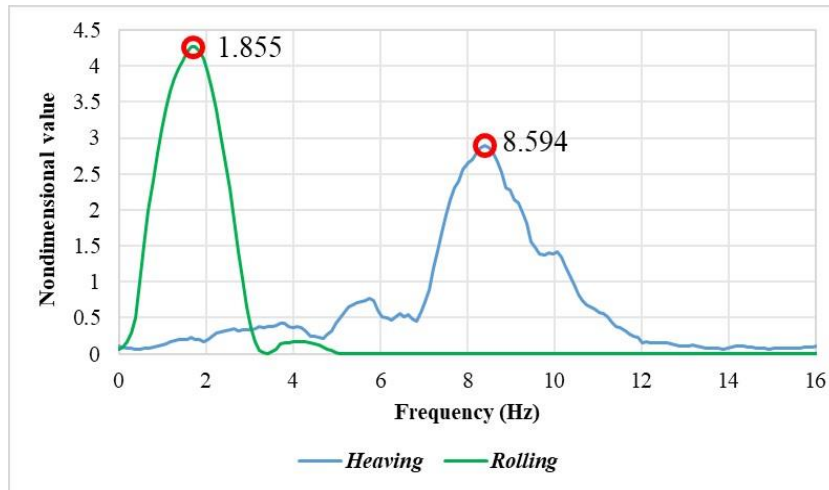


Fig. 3 Heaving and rolling frequencies after FFT

5. Results

5.1 Manual Control Experiment

The experiment aim is controlling the car manually to enable the car to rotate continuously at a randomly chosen but steady turning angle. The car speed gradually increases until rollover occurs.

Data collected by the motion sensor are time-series domain. After the FFT (Fast Fourier Transform), the data become frequency domain data. Fig. 3 portrays an example of FFT results. The maximum amplitude

corresponds to the natural frequency of the car.

Therefore, ν is 1.855 Hz; ν' is 8.594 Hz. Furthermore, the calculated q_{max} is 0.295 g. The relation between q and q_{max} corresponds to the motion states, as Fig. 4 shows. As the speed increases, the lateral force on the car also increases. The body tilts outward gradually. When q reaches q_{max} , the car does not roll over immediately, it merely loses control. For that reason, after the intersection point, the figure of q fluctuates dramatically. Without intervention, the car rolls over after losing control for a while.

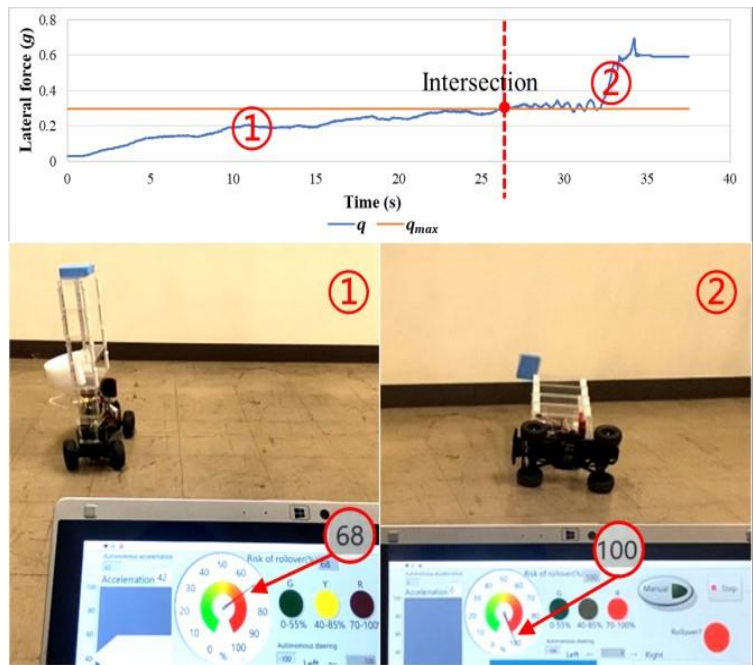


Fig. 4 Lateral force condition between q and q_{max} corresponding to the motion state.

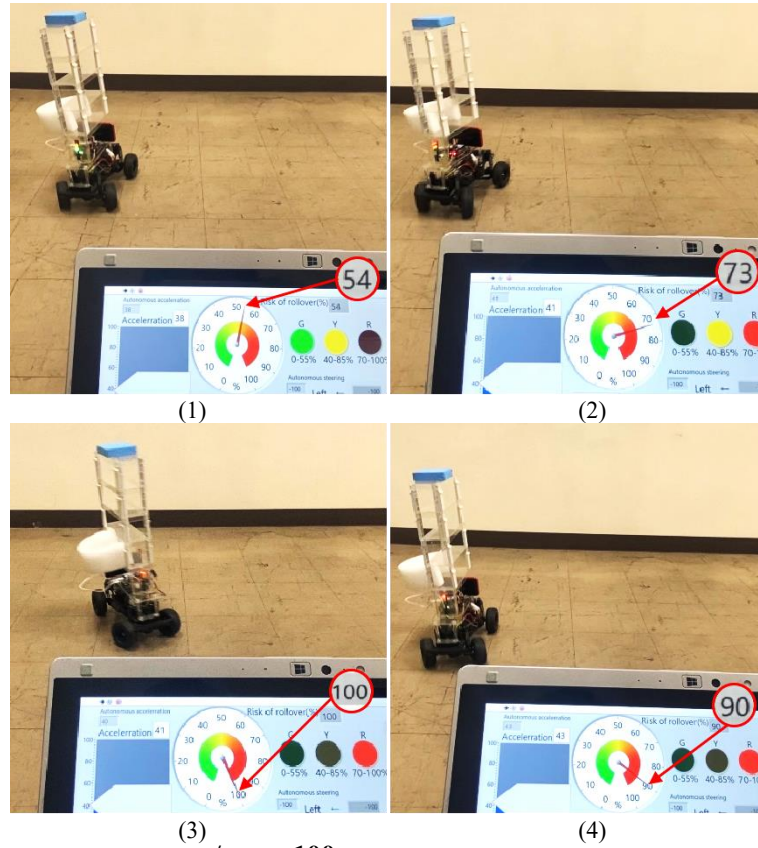


Fig. 5 State of motion and risk of rollover ($q/q_{\max} \times 100$) for a car with delicate speed control: (1) accelerating at lower speed, (2) accelerating at higher speed, (3) reaching 100% rollover risk, (4) avoiding rollover after deceleration.

Table 1 Results of fastest autonomous cornering preventing rollover.

No.	v' (Hz)	v (Hz)	b (m)	w (m)	h (m)	L (m)	L_{\max} (m)	$q_{s \max}$ (g)	$q_{v \max}$ (g)
Exp. 1	8.800	2.070				0.329	2.201	0.300	13.549
Exp. 2	8.735	1.949				0.345	2.169	0.294	12.145
Exp. 3	9.140	2.110	0.168	0.235	0.120	0.337	2.375	0.293	14.860
Exp. 4	9.334	1.860				0.387	2.477	0.270	12.532
Exp. 5	8.401	2.056				0.315	2.006	0.312	12.428
Mean	-	-	0.168	0.235	0.120	0.343	2.246	0.294	13.103

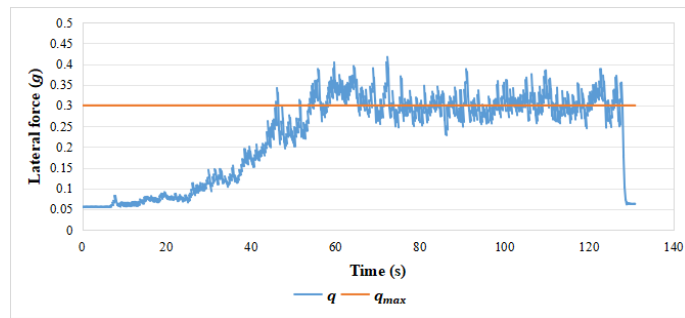
5.2 Experiment of Fastest Autonomous Cornering Preventing Rollover

Fig. 5 presents an illustration of the process of fastest autonomous cornering without rollover. For this experiment, the weight is positioned on the top layer. At low speeds, the risk of rollover is minimal, as depicted in Fig. 5(a). As the speed increases, so does the real-time lateral force. The rollover risk increases as presented in Fig. 5(b). The car continues to accelerate. When the risk reaches 100% as portrayed in

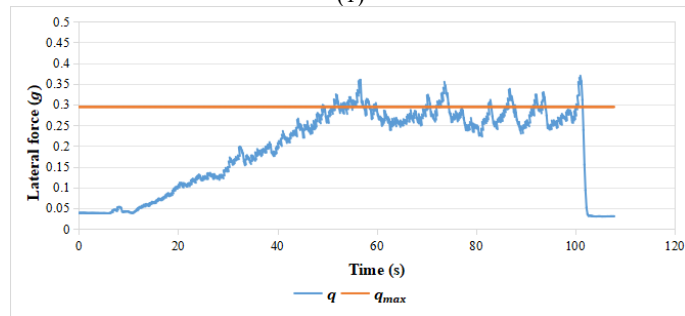
Fig. 5(c), the autonomous cornering system issues a command to decelerate to avoid rollover. After deceleration, the motion state returns to Fig. 5(d). Then the process portrayed in Fig. 5(c), and Fig. 5(d) repeats cyclically. The speed oscillates near the critical rollover threshold, yet rollover never occurs.

The fastest autonomous cornering experiment was conducted five times. Table 1 displays the calculated results.

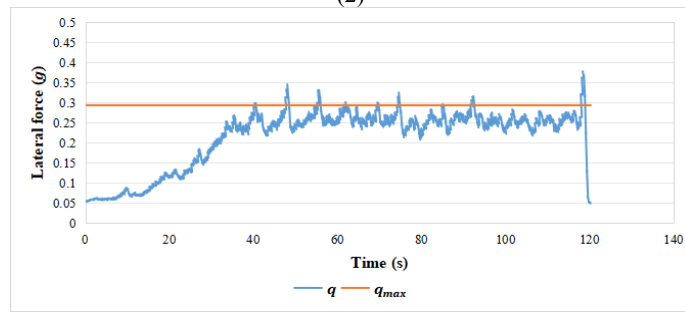
Fig. 6 presents an illustration of the relation between q and q_{\max} during autonomous cornering.



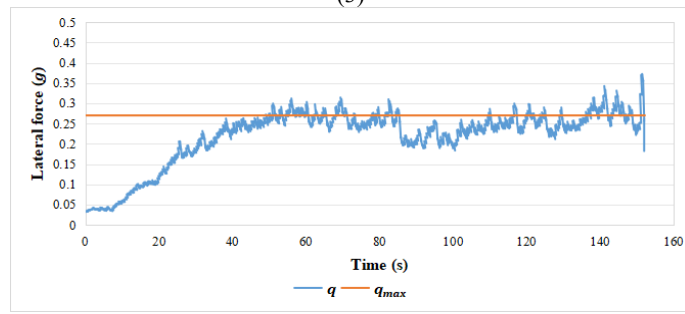
(1)



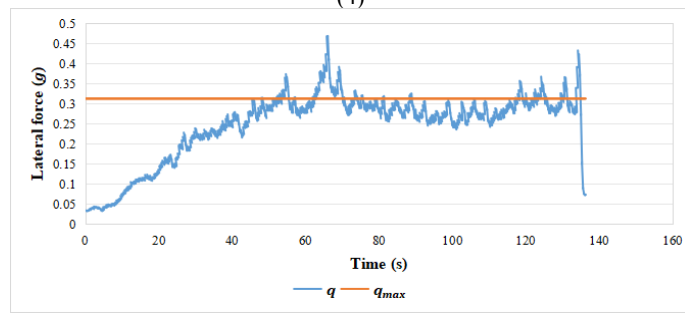
(2)



(3)



(4)



(5)

Fig. 6 Comparison between q and q_{max} for five experiment iterations assessing autonomous cornering preventing rollover.

Initially, along with acceleration of the car, the real-time lateral force also intensifies. Therefore, q demonstrates a general upward trajectory, albeit with some fluctuations. The loading condition remains unchanged; consequently, q_{\max} remains constant.

The shapes of the experimentally obtained results differ, yet they are similar. Every line of q exhibits marked peaks that signify the variation in lateral force resulting from changes in the current. When q reaches q_{\max} , it can be expected to decrease immediately. However, in Fig. 6, because of the characteristics of PD (Proportional Deviation) control, sometimes q continues to increase even if it has exceeded q_{\max} . Similarly, even when q has already fallen below q_{\max} , its decline persists. The car initially loses control rather than rolling over once the value of q reaches its maximum threshold, q_{\max} . Consequently, the autonomous cornering system can avert a rollover promptly.

Aside from the reason presented above, some causes remain for different changes of q , even for identical loading conditions. First, the battery supplies an unstable current, which affects subsequent adjustments to the flow. Secondly, the remote-controlled car scale is quite small. It is therefore susceptible to influences from the ground surface. In fact, even minor disturbances can affect the results detected. Thirdly, before each experiment, the weight is reset. Subtle variations in the positioning of the weight can produce variations in the detection data.

6. Discussion

The primary purpose of this research is development of an effective strategy for preventing vehicle rollover accidents. In a static state, stability depends on the COG height. As the COG elevation increases, the vehicle becomes progressively more susceptible to rollover incidents [6]. To quantify this relation, natural vibration frequencies, including the heaving and rolling frequencies, are incorporated into calculation of the

COG height [17, 18]. Furthermore, the maximum height of the COG is calculated as the static rollover criterion.

When considering dynamic scenarios, particularly during cornering maneuvers, vehicle stability becomes considerably more complex. Lateral force plays a pivotal role in determining the dynamic stability [11]. Multiple factors contribute to the magnitude of the lateral force, including but not limited to the following: the vehicle's cornering speed [4], the curve radius [3], and the COG height [5]. This study introduces an innovative approach by proposing real-time lateral force calculation during cornering operations, along with a dynamic rollover criterion defined as the maximum lateral force before rollover initiation occurs.

The research methodology incorporates a manual control experiment designed to validate the theoretical framework. For this experiment, the cornering speed is increased while maintaining a constant curve radius and COG height parameters. This progressive acceleration leads to corresponding increases in both lateral force and rollover risk. Observations made during experimentation confirm that when the real-time lateral force reaches the predetermined dynamic rollover threshold, the vehicle exhibits distinct shaking behavior preceding the actual rollover occurrence.

During the subsequent experiment particularly addressing autonomous cornering at maximum speed while preventing rollover, the system demonstrated remarkable effectiveness. Although certain environmental and detection variables occasionally influenced the accuracy of the experimentally obtained results, the autonomous cornering system consistently maintained its rollover prevention capability. It is noteworthy that, throughout the entire series of tests, not a single rollover incident occurred. These consistently positive findings constitute compelling evidence for the reliability and precision of this autonomous cornering technology for mitigating rollover risks effectively.

7. Strengths and Limitations

The key strength of this research lies in its innovative approach to rollover prevention by directly analyzing and controlling the vehicle's motion dynamics. Unlike conventional methods that rely on multiple vehicle-specific parameters such as load distribution, suspension characteristics (e.g., spring constants), or tire properties, the model presented in this study merely requires the width of the total weight-bearing section as the fundamental input. Real-time detection can reduce the calculation error to ensure the rollover prevention effectiveness. Another noteworthy benefit of this method is its cost-effectiveness. The equipment and sensor used for this method are affordable and widely available, making the system highly feasible for large-scale implementation across different vehicle types, including commercial trucks, SUVs, and autonomous vehicles. Given its low-cost hardware requirements, computational efficiency, and high reliability, this approach holds strong potential for widespread adoption.

This study also has some limitations which must be acknowledged to guide future research and practical applications. First, the main limitation of this study is the scale of the experiment setup and its potential implications for real-world applications. The research was conducted using a greatly reduced 1/14 scale vehicle model. Although the scaled-down model provides some valuable insights and allows for controlled experimentation, it cannot fully replicate the complex dynamics and performance characteristics of full-sized vehicles in actual operating conditions. Secondly, all experiments are performed on flat, uniform tiled flooring, which fails to replicate many complexities of real-world road surfaces. In practice, asphalt and concrete roads feature varying coefficients of friction, surface irregularities, and superelevation on curved sections, all of which influence vehicle stability. Additionally, road camber, potholes, and uneven terrain can affect stability, but they are not

addressed in this model. Furthermore, this study assumes ideal dry-weather driving conditions, neglecting the effects of rain, snow, ice, and strong winds (e.g., typhoons). Adverse weather alters tire-road friction, vehicle dynamics, and rollover thresholds to a considerable degree. Finally, this system prevents rollover incidents primarily by slowing the vehicle, whereas effectiveness of controlled settings might introduce new risks in actual traffic. For instance, abrupt speed reduction can lead to rear-end collisions if following vehicles do not maintain a safe distance.

8. Evaluation for Fastest Autonomous Cornering Preventing Rollover Demonstrated to Safety Experts of Vehicles

The first author participated in the SSTDC (Student Safety Technology Design Competition) of the 27th International Technical Conference on the Enhanced Safety of Vehicles 2023 [20]. A scale model of the fastest autonomous cornering preventing rollover based on D3DCG was demonstrated and presented at the conference for four days to safety experts of vehicles from all over the world. First place of the SSTDC was awarded to the author at that conference.

9. Conclusions

This research has demonstrated a real-time and precise method to prevent rollover based on the relation between motions and position of the center of gravity. Only a motion sensor is necessary to record the motion data of vehicles with no knowledge of the mass and spring constant. Data collection is repeated. The processes of detection and calculation for this research take only a few seconds. Moreover, the results include few errors.

This technology is believed to hold great promise for future applications in real vehicles and autonomous driving, particularly for rollover prevention and the protection of human life.

References

- [1] National Highway Traffic Safety Administration. 2022. "Passenger Car and Light-Truck Occupants Killed, by Vehicle Type and Rollover Occurrence, 1982-2020." <https://cdan.dot.gov/SASJobExecution/>.
- [2] National Highway Traffic Safety Administration. 2010. "Review of NMVCCS Rollover Variables in Support of Rollover Reconstruction." https://www.nhtsa.gov/sites/nhtsa.gov/files/811235_0.pdf.
- [3] Chu, D., Li, Z., Wang, J., Wu, C., and Hu, Z. 2018. "Rollover Speed Prediction on Curves for Heavy Vehicles Using Mobile Smartphone." *Measurement* 130: 404-11.
- [4] Fan, L., Li, G., Chen, R., Hu, D., Zhao, L., and Hu, L. 2016. "Speed Calculation Model and Simulation of rollover Prevention in Condition of Extreme Turn Based on Lateral Force Coefficient." *Transactions of the Chinese Society of Agricultural Engineering* 32 (3): 41-7.
- [5] Yang, Y., and Qiu, X. 2019. "The Conditions and Influencing Factors of Trucks' Roll-Over during Turning." *Mechanics in Engineering* 41 (4): 393-7.
- [6] Lang, M., Peng, Y., and Liu, C. 2010. "Influence of Gravity Center Height on Running Safety of Loaded Double-Stack Container Car." *Journal of Traffic and Transportation Engineering* 10 (6): 41-7.
- [7] Chen, B., and Peng, H. 1999. "Rollover Warning of Articulated Vehicles Based on a Time-To-Rollover Metric." In *The ASME 1999 International Mechanical Engineering Congress and Exposition*, pp. 247-54.
- [8] Larish, C., Piyabongkarn, D., Tsourapas, V., and Rajamani, R. 2013. "A New Predictive Lateral Load Transfer Ratio for Rollover Prevention Systems." *IEEE Transactions on Vehicular Technology* 62 (7): 2928-36.
- [9] Bharane, P., Tanpure, K., Patil, A., and Kerkal, G. 2014. "Design, Analysis and Optimization of Anti-Roll Bar." *International Journal of Engineering Research and Applications* 4 (9): 137-40.
- [10] Zhu, B., Piao, Q., Zhao, J., and Guo, L. 2016. "Integrated Chassis Control for Vehicle Rollover Prevention with Neural Network Time-To-Rollover Warning Metrics." *Advances in Mechanical Engineering* 8 (2): 1-13.
- [11] Li, H., Zhao, Y., Wang, H., and Lin, F. 2017. "Design of an Improved Predictive LTR for Rollover Warning Systems." *Journal of the Brazilian Society of Mechanical Sciences and Engineering* 39: 3779-91.
- [12] Yim, S., Jeon, K., and Yi, K. 2012. "An Investigation into Vehicle Rollover Prevention by Coordinated Control of Active Anti-Roll Bar and Electronic Stability Program." *International Journal of Control, Automation and Systems* 10 (2): 275-87.
- [13] Gaspar, P., Szabo, Z., and Bokor, J. 2005. "Brake Control Combined with Prediction to Prevent the Rollover of Heavy Vehicles." *IFAC Proceedings* 38 (1): 248-53.
- [14] He, J., Gong, B., Zhu, T., Yang, C., and Sun, Y. 2017. "Critical Safety Speed Model of Corners Based on Road Geometry Parameters." *Journal of Changsha University of Science and Technology: Natural Science* 14 (4): 75-82.
- [15] Solmaz, S., Akar, M., and Shorten, R. 2008. "Adaptive Rollover Prevention for Automotive Vehicles with Differential Braking." *IFAC Proceedings* 41 (2): 4695-700.
- [16] Mikata, Y., Yamanaka, M., Kameoka, K., Okunosono, A., and Kinoshita, T. 2011. "Measuring the Center of Gravity with Truck Scale." In *The SICE Annual Conference*, pp. 405-10.
- [17] Dang, R., and Watanabe, Y. 2016. "Three-Dimensional Center of Gravity for Trucks Hauling Marine Containers." *International Journal of Engineering Research and Applications* 6 (1): 27-34.
- [18] Watanabe, Y. 2017. "Three-Dimensional Center of Gravity Detections for Preventing Rollover Accidents of Trailer Trucks Hauling Containers." *Open Journal of Mechanical Engineering* 2 (1): 11-4.
- [19] Kawashima, S., and Watanabe, Y. 2012. "Experiment on The Three Dimensional Detection of Center of Gravity for Detecting Deterioration of Automobile Tire." In *The Japan Society of Mechanical Engineers*, pp. 161-4.
- [20] Yu, K., Xu, S., and Onodera, M. 2023. "Fast Autonomous Cornering Without Causing Rollover Based on the Detection of Three-Dimensional Center of Gravity (D3DCG)." In *Student Safety Technology Design Competition of the 27th Enhanced Safety of Vehicles International Conference*. https://www.mlit.go.jp/en/report/press/jidosha10_hh_000002.html, <https://www.esv.nhtsa.dot.gov/>.